Dalton Transactions

COMMUNICATION

View Article Online
View Journal

Check for updates

Cite this: DOI: 10.1039/c7dt03854b

Received 13th October 2017,
Accepted 28th November 2017

DOI: 10.1039/c7dt03854b

rsc.li/dalton

$Li_6Na_3Sr_{14}Al_{11}P_{22}O_{90}$: an oxo-centered Al_3 cluster based phosphate constructed from two types of (3,6)-connected kgd layers†

Xiao-Ni Yao,[a] Yi-Gang Chen,*[a] Yao Guo,[b] Ying-Jie Jia,[a] Xing-Xing Jiang[c] and Xian-Ming Zhang*[a]

A novel and thermally stable aluminum phosphate $Li_6Na_3Sr_{14}Al_{11}P_{22}O_{90}$ (1) has been achieved by using a solid-state molten method, which contains an oxo-centered trinuclear cluster and an anti-Lowenstein's rule Al–O–Al linkage and is constructed from two types of (3,6)-connected kgd layers $[Al(Al_3O)(PO_4)_7]^{25-}$ and $[Al(PO_4)_2]^{3-}$. The good optical transparency in the whole UV range and excellent thermal stability make the title compound a potential optical window material.

Aluminophosphates (AlPOs) have long attracted much attention owing to their rich structures[1] and optical properties as well as wide applications in catalysis, adsorption, separation, and ion exchange.[2] Since a new class of zeolite-like $AlPO_{4-n}$ molecular sieves was developed at the beginning of the 1980s,[3] more than 200 aluminophosphate structures have been prepared by using hydrothermal, solvothermal or ionothermal synthetic techniques.[4]

From the viewpoint of the primary building block, AlPOs are made up of alternate Al-centered polyhedra (three kinds: AlO_4, AlO_5, and AlO_6) and P-centered tetrahedra $P(O_b)_n(O_t)_{4-n}$ (b: bridging, t: terminal, n = 1, 2, 3, and 4),[5] which have contributed to fruitful structures and compositions of AlPOs. In light of the electrostatic properties, AlPOs can be classified into neutral framework $AlPO_4$–n with Al/P = 1 and anionic framework AlPOs with Al/P < 1.[6] As far as bonding patterns are concerned, almost all the AlPOs obey Lowenstein's rule[7] and avoid Al–O–Al bonds.

It is also revealed that inorganic cations and organic templates have a great effect on the frameworks of AlPOs.[8] For example, in terms of the M–AlPO system, anionic framework compounds with different dimensionalities such as 3D $NaCs_2Al(PO_4)_2$, 2D $NaRb_2Al_2(PO_4)_3$ [9] and 1D $RbAl_3(P_3O_{10})_2$ [10] chains have been observed. However, the organic templates often result in poor thermal stability. As can be seen, it remains a big challenge to synthesize novel and thermally stable AlPOs with the anti-Lowenstein's rule Al–O–Al linkage. To overcome the above limitations, a high temperature organic-free template solid-state molten method is used herein to synthesize novel AlPOs with good thermal stability. Moreover, alkali and alkaline-metal cations contribute to ultraviolet (UV) light transmission due to the absence of d–d electron transition.[11]

Herein we present the solid-state molten synthesis of a novel aluminophosphate $Li_6Na_3Sr_{14}Al_{11}P_{22}O_{90}$ (**1**), which contains an oxo-centered trinuclear aluminum cluster with the anti-Lowenstein's rule Al–O–Al linkage and is constructed from two types of (3,6)-connected kgd[12] layers $[Al(PO_4)_2]^{3-}$ and $[Al(Al_3O)(PO_4)_7]^{25-}$. In addition, thermo-stability, X-ray diffraction, optics and band structure from density functional theory (DFT) were studied.

The colorless and transparent single crystals of **1** (Fig. S1†) were obtained in platinum crucibles by melting the mixtures of $Na_2CO_3/SrF_2/LiF/Al_2O_3/NH_4H_2PO_4$ at a molar ratio of 2 : 3 : 4 : 2 : 8. The purity of the crystal was proved by powder X-ray diffraction (XRD) analysis (Fig. S2†). Inductively coupled plasma elemental analysis provided a molar ratio of 5.76 : 3.20 : 13.81 : 10.86 : 21.98 for Li, Na, Sr, Al, and P atoms, respectively, corresponding to the formula sum from single-crystal XRD analysis. Bond valence calculations[13] (Li, 0.806–1.011; Na, 1.177–1.299; Sr, 1.932–2.109; Al, 2.745–2.926; P, 4.993–5.211; O, 1.804–2.149) demonstrate that the Li, Na, Sr, Al, P, and O atoms are in the expected oxidation states of +1, +1, +2, +3, +5 and −2, respectively.

The most remarkable feature of **1** is that it is unprecedentedly composed of two types of (3,6)-connected kgd layers $[Al(PO_4)_2]^{3-}$ and $[Al(Al_3O)(PO_4)_7]^{25-}$. The kgd net topology is the kagome dual net topology; the point symbol of the 2D (3,6)-connected kgd-type topology is represented as $(4^3)_2(4^6{\cdot}6^6{\cdot}8^3)$.

[a]Key Laboratory of Magnetic Molecules and Magnetic Information Material of Ministry of Education, School of Chemistry and Material Science, Shanxi Normal University, Linfen, 041004, China. E-mail: yg_chen80@sina.com, zhangxm@dns.sxnu.edu.cn

[b]Department of Chemical and Environmental Engineering, Anyang Institute of Technology, Anyang 455000, China

[c]Beijing Center for Crystal Research and Development, Key Laboratory of Functional Crystals and Laser Technology, Technical Institute of Physics and Chemistry, Chinese Academy of Sciences, Beijing 100190, China

† Electronic supplementary information (ESI) available: Experimental procedures and characterisation data for compound **1**. CCDC 1563911. For ESI and crystallographic data in CIF or other electronic format see DOI: 10.1039/c7dt03854b

The $[Al(PO_4)_2]^{3-}$ 2D sheet can be seen as a kgd network by simplifying the PO_4 tetrahedron as a 3-connecting node and the AlO_6 octahedron as a 6-connecting node, while the (3,6)-connected $[Al(Al_3O)(PO_4)_7]^{25-}$ 2D kgd layer is based on the $Al_3O(PO_4)_7$ cluster as a 3-connected node and the $Al(1)O_6$ octahedron as a 6-connected node. Compound **1** crystallizes in the monoclinic space group of $C_{2/m}$ (no. 12), and the asymmetric unit (Fig. S3†) consists of crystallographically distinct 3 Li, 2 Na, 5 Sr, and 5 Al atoms and 8 PO_4 groups. The Al(3) and Al(4) atoms show octahedral AlO_6 coordination geometries, which are linked by μ_3-PO_4 groups *via* corner-sharing oxygen to complete the 2D anionic $[Al(PO_4)_2]^{3-}$ layer[14] (Fig. 1a). From the topological point of view, the layer can be simplified as a (3,6)-connected kgd topology (Fig. 1b).

The unique $[Al(Al_3O)(PO_4)_7]^{25-}$ layer contains oxo-centered trinuclear aluminum clusters and has never been documented in AlPOs to date. There are three independent Al sites in the $[Al(Al_3O)(PO_4)_7]^{25-}$ layer. Al(1) localizes at the crossing point of the mirror plane and two-fold axis and has a site occupancy of 0.25 (Wyck. 2b); Al(2) localizes at the mirror plane and has a site occupancy of 0.5 (Wyck. 4i). Two square pyramidal Al(5) and one octahedral Al(2) atoms *via* sharing the μ_3-O(22) atom form an oxo-centered isosceles trinuclear Al_3O unit with Al···Al distances of 3.0658 and 3.2371 Å and Al–O–Al angles of 115.93°–121.586(1)°. Each Al_3O unit is surrounded by seven phosphates to form trinuclear $Al_3O(PO_4)_7$ clusters where six phosphates are bridged and one phosphate is terminal (Fig. 1c). Each $Al(1)O_6$ octahedron is linked to six $Al_3O(PO_4)_7$ clusters while each $Al_3O(PO_4)_7$ cluster is linked to only three $Al(1)O_6$ octahedra, resulting in a $[Al(Al_3O)(PO_4)_7]^{25-}$ layer (Fig. 1d) also with the (3,6)-connected kgd topology (Fig. 1b). The thickness of the $[Al(Al_3O)(PO_4)_7]^{25-}$ layer is approximately two times that of the $[Al(PO_4)_2]^{3-}$ layer (Fig. 2a).

What should be of concern is that the anti-Lowenstein's rule[15] and energetically unfavorable Al–O–Al linkages exist in an oxo-centered isosceles trinuclear Al_3O unit of compound **1**. This differs from almost all known AlPOs that obey the Lowenstein's rule and avoid Al–O–Al bonds.[16] It is possible that energetically unfavorable anti-Lowenstein Al–O–Al direct linkages in **1** could be overcome by high temperature.[17]

Two crystallographically distinct Na atoms are nine- and eight-coordinated with O atoms. And three crystallographically unique Li atoms, Li(1), Li(2), and Li(3), are four-, three-, and four-coordinated with O atoms, respectively (Fig. S4†). Li and Na atoms are alternately located at the grooves inside the $[Al(PO_4)_2]^{3-}$ and $[Al(Al_3O)(PO_4)_7]^{25-}$ layers (Fig. 2b), with the Li–O and Na–O bond distances in the range of 1.982(14)–2.417(14) Å and 2.133(14)–2.710(6) Å, respectively. Five Sr atoms including dually disordered Sr(5) possess three cooperative coordination modes SrO_n (n = 8, 11 and 12) with bond lengths of 2.403(9)–3.063(2) Å (Fig. S5†). These Sr atoms are housed not only within the $[Al(Al_3O)(PO_4)_7]^{25-}$ layers but also in the interval of $[Al(PO_4)_2]^{3-}$ and $[Al(Al_3O)(PO_4)_7]^{25-}$ layers as shown in Fig. 2b. From the perspective of cation distribution, the smaller cations Li^+ and Na^+ act mainly as the charge compensators while the bigger ions of Sr^{2+} with more charges within the interlayers play both structure-directing and charge compensating roles.

Thermal behavior analysis (Fig. 3a) shows that compound **1** has a good thermal stability with a melting point of 846 °C. UV transmittance spectra show that their UV cutoff edge is up to 230 nm with a band gap of about 4.78 eV (Fig. 3b), suitable

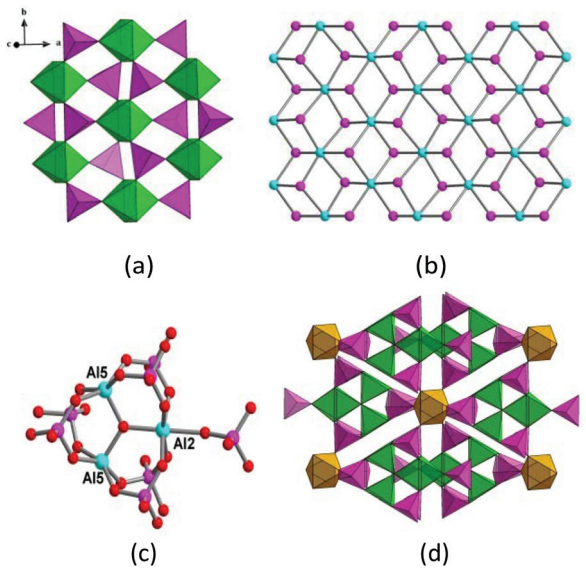

Fig. 1 (a) 2D anionic $[Al(PO_4)_2]^{3-}$ layer, purple and green polyhedra represent PO_4 and AlO_6, respectively; (b) (3,6)-connected kgd topology; (c) the novel trinuclear $Al_3O(PO_4)_7$ cluster; (d) the unique $[Al(Al_3O)(PO_4)_7]^{25-}$ layer. Each orange $Al(1)O_6$ octahedron is linked to six $Al_3O(PO_4)_7$ clusters.

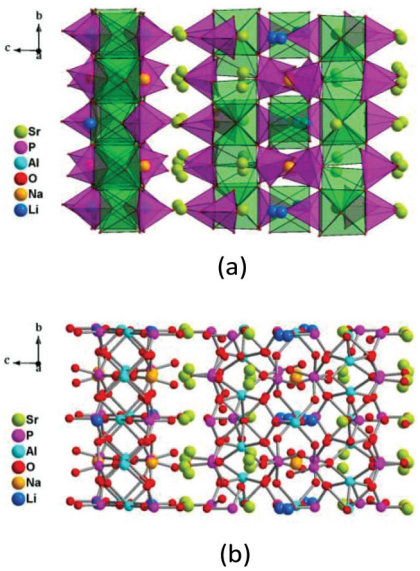

Fig. 2 (a) The thickness of the $[Al(Al_3O)(PO_4)_7]^{25-}$ layer is about two times that of the $[Al(PO_4)_2]^{3-}$ layer; (b) the fill-style of cations Sr^{2+}, Li^+ and Na^+ in the $[Al(PO_4)_2]^{3-}$ and $[Al(Al_3O)(PO_4)_7]^{25-}$ layers.

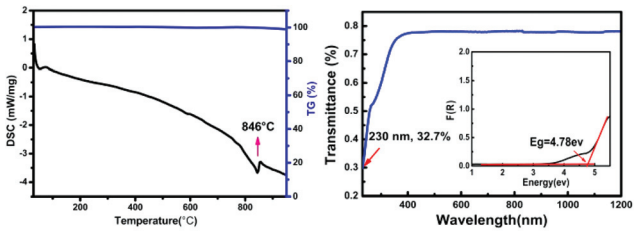

Fig. 3 (a) TGA and DSC curves of compound **1** with a melting point of 846 °C; (b) UV-vis-IR spectra of compound **1**, the UV cutoff edge is up to 230 nm with a band gap of about 4.78 eV.

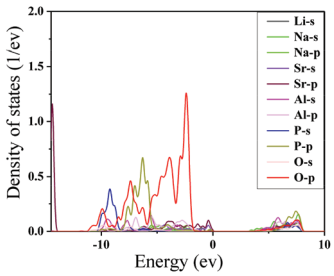

Fig. 4 Density of states (DOS) based on DFT methods.

for UV optical applications.[18] The electronic band structure and density of states (DOS) based on DFT methods were calculated to further explore the crystal and optical property relationship. The band structure (Fig. S7†) indicates that **1** is a direct-band-gap crystal with a calculated value of 3.52 eV, smaller than that of the experimental result because of the limitation of the DFT method. The DOS (Fig. 4) suggests that the valence band (VB) from −8.0 eV to the maximum consists mainly of the O 2p, P 3p, Al 3s 3p, and little Sr 5s orbitals, whereas the conduction band (CB) bottom contains all the constituent atomic orbitals. The optical properties derived mostly from electronic transitions between the VB and CB are close to the band gap, such that the bonding interactions between O and P, Al, Sr, Li and Na determine the optical response of **1**.

In conclusion, a new aluminum phosphate crystal **1** with good thermal stability has been synthesized by controlling different alkali metals and alkaline-earth metal ions. It contains an oxo-centered trinuclear aluminum cluster with an anti-Lowenstein's rule Al–O–Al linkage and is constructed from two types of (3,6)-connected kgd layers $[Al(PO_4)_2]^{3-}$ and $[Al(Al_3O)(PO_4)_7]^{25-}$. The good optical transparency in the whole UV range and excellent thermal stability make the title compound a potential optical window material.

Conflicts of interest

There are no conflicts to declare.

Acknowledgements

This work was financially supported by the Plan for 10000 Talents in China, the National Science Fund for Distinguished Young Scholars (20925101), the Shanxi Province Foundation for Key Subject and the National Natural Science Foundation of China (Grant No. 21406134).

References

1 (*a*) J. Chyba, Z. Moravec, M. Necas, S. Mathur and J. Pinkas, *Inorg. Chem.*, 2014, **53**, 3753–3762; (*b*) D. M. Dawson and S. E. Ashbrook, *J. Phys. Chem. C*, 2014, **118**, 23285–23296; (*c*) R. H. Jones, J. M. Thomas, R. Xu, Q. Huo, A. K. Cheetham and A. V. Powell, *J. Chem. Soc., Chem. Commun.*, 1991, **18**, 1266–1268; (*d*) Y. Li and J. Yu, *Chem. Res.*, 2014, **114**, 7268–7316; (*e*) C. Liu, W. Yang, N. Qu, L. J. Li, Q. J. Pan and Z. M. Sun, *Inorg. Chem.*, 2017, **56**, 1669–1678; (*f*) L. Shao, Y. Li, J. Yu and R. Xu, *Inorg. Chem.*, 2012, **51**, 225–229; (*g*) Z. Xia and K. R. Poeppelmeier, *Acc. Chem. Res.*, 2017, **50**, 1222–1230; (*h*) W. Yang, H. Y. Wu, R. X. Wang, Q. J. Pan, Z. M. Sun and H. Zhang, *Inorg. Chem.*, 2012, **51**, 11458–11465.

2 (*a*) D. M. Dawson, J. M. Griffin, V. R. Seymour, P. S. Wheatley, M. Amri, T. Kurkiewicz, N. Guillou, S. Wimperis, R. I. Walton and S. E. Ashbrook, *J. Phys. Chem. C*, 2017, **121**, 1781–1793; (*b*) M. E. Potter, A. J. Paterson, B. Mishra, S. D. Kelly, S. R. Bare, F. Corà, A. B. Levy and R. Raja, *J. Am. Chem. Soc.*, 2015, **137**, 8534–8540; (*c*) H. E. van der Bij, D. Cicmil, J. Wang, F. Meirer, F. M. F. de Groot and B. M. Weckhuysen, *J. Am. Chem. Soc.*, 2014, **136**, 17774–17787; (*d*) L. Gómez-Hortigüela, F. Corà and C. R. A. Catlow, *ACS Catal.*, 2011, **1**, 1487–1497; (*e*) B. T. Holland, P. K. Lsbester, C. F. Blanford, E. J. Munson and A. Stein, *J. Am. Chem. Soc.*, 1997, **119**, 6796–6803; (*f*) W. Yan, E. W. Hagaman and S. Dai, *Chem. Mater.*, 2004, **16**, 5182–5186.

3 T. W. Stephen, B. M. Lok, A. M. Celeste, R. C. Thomas and M. F. Edith, *J. Am. Chem. Soc.*, 1982, **104**, 1146–1147.

4 (*a*) D. S. Belén-Cordero, C. Kim, S. J. Wang and A. J. Hernández Maldonado, *J. Phys. Chem. C*, 2009, **113**, 8035–8049; (*b*) E. R. Parnham and R. E. Morris, *J. Am. Chem. Soc.*, 2006, **128**, 2204–2205; (*c*) X. Zhao, J. Zhao, C. Y. Chang, Z. Li, Y. Zhao and W. Zhou, *New J. Chem.*, 2016, **40**, 2444–2450; (*d*) Z. Liu, X. Song, J. Li, Y. Li, J. Yu and R. Xu, *Inorg. Chem.*, 2012, **51**, 1969–1974.

5 J. Yu and R. Xu, *Chem. Soc. Rev.*, 2006, **35**, 593–604.

6 J. Yu and R. Xu, *Acc. Chem. Res.*, 2003, **36**, 481–490.

7 W. Lowenstein, *Am. Mineral.*, 1954, **39**, 92.

8 (*a*) L. Gómez-Hortigüela, C. Márquez Álvarez, F. Corà, F. López-Arbeloa and J. Pérez Pariente, *Chem. Mater.*, 2008, **20**, 987–995; (*b*) Z. Han, A. L. Picone, A. M. Z. Slawin, V. R. Seymour, S. E. Ashbrook, W. Zhou, S. P. Thompson, J. E. Parker and P. Wright, *Chem. Mater.*, 2010, **22**, 338–346.

9 Q. H. Wu and S. J. Chen, *Chem. Mater.*, 2001, **13**, 1794–1799.
10 J. Lesage, A. Guesdon and B. J. Raveau, *Solid State. Chem.*, 2005, **178**, 1212–1220.
11 (*a*) Y. G. Chen, M. L. Xing, P. F. Liu, Y. Guo, N. Yang and X. M. Zhang, *Inorg. Chem.*, 2017, **56**, 845–851; (*b*) S. Wang, N. Ye and G. Zou, *Inorg. Chem.*, 2014, **53**, 2742–2748.
12 (*a*) J. P. Zou, Q. Peng, Z. Wen, G. S. Zeng, Q. J. Xing and G. C. Guo, *Cryst. Growth Des.*, 2010, **10**, 2613–2619; (*b*) J. J. Hou, X. Q. Li, P. Gao, H. Q. Sun and X. M. Zhang, *Cryst. Growth Des.*, 2017, **17**, 3724–3730; (*c*) L. Y. Cao, Z. K. Lin, W. J. Shi, Z. Wang, C. K. Zhang, X. F. Hu, C. Wang and W. B. Lin, *J. Am. Chem. Soc.*, 2017, **139**, 7020–7029.
13 I. D. Brown and D. Altermatt, *Acta Crystallogr., Sect. B: Struct. Sci.*, 1985, **41**, 244–247.
14 (*a*) S. C. Kim, H. J. Kwak, C. Y. Yoo, H. Yun and S. J. Kim, *J. Solid State Chem.*, 2016, **243**, 12–17; (*b*) K. J. R. Morgan, G. B. Gainsford and N. Milestone, *Chem. Commun.*, 1997, 61–62.
15 Q. Huang and S. J. Hwu, *Chem. Commun.*, 1999, 2343–2344.
16 J. L. Provis, P. Duxson, G. C. Lukey and J. S. J. van Deventer, *Chem. Mater.*, 2005, **17**, 2976–2986.
17 R. G. Bell, R. A. Jackson and C. R. A. Catlow, *Zeolites*, 1992, **12**, 870–871.
18 Y. Wang, S. Pan, S. Han, L. Dong, M. Zhang and K. Wu, *New J. Chem.*, 2014, **38**, 889–892.

